Food Research 7 (Suppl. 2) : 78 - 82 (2023)
Journal homepage: https://www.myfoodresearch.com

FOOD RESEARCH

FULL PAPER

Sago pith waste: morphology, chemical composition and thermal properties

[1,*]Yacob, N., [2]Badri, K. and [3]Mohamed, A.Z.

[1]*Malaysian Nuclear Agency (Nuclear Malaysia), Bangi, 43000 Kajang, Malaysia*
[2]*Faculty of Science and Technology, Universiti Kebangsaan Malaysia, 43600 Bangi, Selangor, Malaysia*
[3]*Institute of Tropical Forestry and Forest Products (INTROP), Universiti Putra Malaysia, 43400 UPM Serdang, Selangor, Malaysia*

Article history:
Received: 1 September 2022
Received in revised form: 19 October 2022
Accepted: 22 October 2022
Available Online: 25 September 2023

Keywords:
Sago pith waste,
Chemical composition,
Hemicellulose,
Cellulose,
Lignin

DOI:
https://doi.org/10.26656/fr.2017.7(S2).13

Abstract

Comprehensive knowledge of the chemical components in the sago pith waste will facilitate the use of the materials in agricultural industrial sector and help to enhance their utilization in the chemical and biochemical related industry. This paper studied the chemical composition especially extractives, hemicellulose, α-cellulose, lignin and ash content as well as morphological and thermal properties of sago pith waste. The chemical compositions of sago pith waste were determined in accordance with the standard outlined in TAPPI test methods. The results revealed that the mean cellulose, hemicellulose and lignin values were 14.32, 17.45 and 4.83% respectively. FTIR spectra confirmed the presence of functional groups that represented cellulose, hemicellulose and lignin. Morphological observation showed that the average size of sago pith waste was 300-600 µm with sago starch granules were seen entrapped in parenchyma cells. Based on the results, sago pith waste can be used as a non-wood renewable source for other applications.

1. Introduction

Efforts have been made to replace petroleum-based products by replacing them with biomass feedstock. The use of agro-waste fibers would result in partial degradation of unused products. The consideration of using these fibers is based on their contribution to the utilization of plant waste and the availability of fibers abundantly. The reuse of these residues helps in solving environmental problems, especially in the volume of waste accumulated in the environment. One of the alternatives to reduce agro-waste disposal is converting it to high-end value products. Among agro-waste abundantly available in Malaysia are palm-based biomass like oil palm (*Elaeis* sp.), sugar palm (*Arenga* sp.) and sago palm (*Metroxylon* sp.).

Sago palm is widely found in Indonesia, Philippines, Malaysia, Papua New Guinea, Thailand and Vietnam. In Malaysia, 90% of the sago planting area is found in Sarawak and Mukah is the largest sago producer in Sarawak where over 50% of sago starch is produced (Bujang and Ahmad, 1999). It grows well in swampy areas, peat soils, dry soils and acidic soils. The sago palm has become one of the most favorable plants because it is economically acceptable, relatively sustainable, environmentally friendly and promotes a socially stable agricultural industry. Unlike other plants that store starch in seeds, roots or tubers, sago starch accumulates in the parenchyma cells in the trunk of the sago tree. Since sago tree trunk stores starch, more than 90% of sago tree stems are parenchyma cells. Singhal *et al.* (2008) reported that sago plantations in Sarawak can produce up to 25 tonnes.ha^{-1} of starch in a year. The residue left behind after sago starch extraction is called sago pith waste. Generally, this residue is used for animal feed, compost for mushroom culture and as raw material in particleboard manufacture (Lai *et al.*, 2014). Further, this sago waste is also processed as a soil improver and natural fertilizer due to the small content of nutrients left in it (Singhal *et al.,* 2008).

To date, a detailed and comprehensive study of the fundamental properties of sago pith waste is still lacking. The knowledge of fiber components, as well as their proportion, enables the selection of sufficient pre-treatment (chemical or mechanical) for the removal of the amorphous and non-cellulosic components. Therefore, this study was conducted to report the characteristics of sago pith waste in terms of its chemical composition, morphology as well and thermal properties.

*Corresponding author.
Email: *norzita@nm.gov.my*

eISSN: 2550-2166
Published by Rynnye Lyan Resources

The objective of this work was to investigate the chemical composition, functional groups, thermal properties and morphology (shape and size) of sago pith waste. Morphological analysis has been carried out using FESEM whereas chemical composition was measured according to TAPPI standard and FTIR spectroscopy as well as elemental analysis by EDX. Meanwhile, thermal property was studied using thermogravimetric analysis (TGA). Hence, the knowledge gained from this study is useful for further applied research study to evaluate the potential of sago pith waste for new applications.

2. Materials and methods

2.1 Materials

Sago waste was obtained from Ng Kia Seng Kilang Sagu Industries Sdn. Bhd. Batu Pahat, Johor. The chemical reagents used were sodium chlorite (purchased from Sigma Aldrich), acetic acid, sodium hydroxide, ethanol, toluene, sulphuric acid (purchased from Fisher Scientific Inc). All the chemical reagents were used as received.

2.2 Determination of chemical composition

Soxhlet extraction with alcohol–benzene (TAPPI T204) was carried out for 6 hrs to calculate the content of the extractive. The percentage of holocellulose was determined according to the method described by Wise *et al.* (1946). The lignin (acid-insoluble) and α-cellulose contents were determined according to TAPPI standard methods T222 and T203, respectively. The ash content was carried out following the T-211 method. Determination of sago residue starch content was conducted using the titration method based on Lane-Eynon method.

2.3 Determination of functional groups using Fourier Transform Infrared Spectroscopy

The FTIR spectra were recorded on a spectrometer model Bruker Tensor II, Germany in the range of 4000-500 cm^{-1} with a scanning resolution of 2 cm^{-1} to investigate the functional groups in sago pith waste.

2.4 Morphological observation of sago pith waste using Field Emission Scanning Electron Microscope

Morphological observation of sago pith waste was conducted using FESEM (Carl Zeiss model Gemini SEM 500). Prior to the scanning process, the samples were coated with platinum to avoid charging.

2.5 Determination of thermal properties using thermogravimetric analysis

Thermal decomposition of sago pith waste was characterized using thermogravimetric analyzer (Perkin Elmer Pyris model 1). Sample between 2-12 mg was weighed and placed into alumina flat. The analysis was carried out at a temperature between 27-600°C with a heating rate of 10°C/min under a nitrogen gas atmosphere at a flow rate of 20 mL/min.

3. Results and discussion

3.1 Chemical composition of sago pith waste

The chemical composition of sago pith waste was determined, and the results are listed in Table 1. It is shown from the table that sago pith waste contains a high amount of sago starch (38.41%). Meanwhile, sago pith waste also contains cellulose (14.31%), hemicellulose (17.45%) and lignin (4.83%). Besides, sago pith waste also contained 2.82% extractive and 2.74% ash. Lower lignin content is normally found in non-wood fibers. Thus, it is easier to remove lignin during extraction. Lignin functions as an adhesive to bind cellulose together in the fiber. Since sago starch is stored in the parenchyma cells of sago tree stem, it is relatively difficult to remove sago starch completely. Granule sago starch which is entrapped within the fibers during starch extraction explains why sago pith waste has a high starch content. According to Kamal *et al.* (2006), the percentage of starch content in sago pith waste depends on the starch extraction technique. Extraction by conventional methods using old equipment makes it difficult to extract sago starch effectively compared to new methods using modern equipment.

3.2 Morphology of sago pith waste

Figure 1(a) displays a photograph of the dried sago pith waste while Figure 1(b) shows a FESEM micrograph of sago pith waste. The dried sago pith waste exhibited a light brown color. The average size of the sago pith waste revealed around 300-600 μm as measured by a particle size analyzer. The sample of sago pith waste displayed a longitudinal structure. The individual fibers are bound together with an average diameter of around 600 μm.

Figure 2 shows a cross-section of sago pith waste. The waste structure is hexagonal and is attached to each other like a honeycomb. The structure is surrounded by a single layer of walls. The space between cells or lumens

Table 1. Chemical composition of sago pith waste.

Sample	Moisture content (%)	Starch (%)	Cellulose (%)	Hemicellulose (%)	Lignin (%)	Extractive (%)	Ash (%)
SW	3.5±0.17	38.41±1.36	14.31±1.48	17.45±0.90	4.83±1.04	2.82±1.36	2.74±0.42

https://doi.org/10.26656/fr.2017.7(S2).13

is surrounded by parenchyma cells. Parenchyma cells in sago trees stored starch in addition to providing support to the tree (Nitta *et al.,* 2006). Residual sago starch granules are still seen indicating that sago starch has not been completely extracted from the trunk of sago trees, but the amount is not significant. Sago starch granules were identified based on the observations shown in the FESEM micrograph (thumbnail Figure 2(a). The sago starch granules are white and oval with sizes between 20 -60 µm in diameter. The presence of sago starch was also supported by chemical analysis as discussed earlier in Table 1.

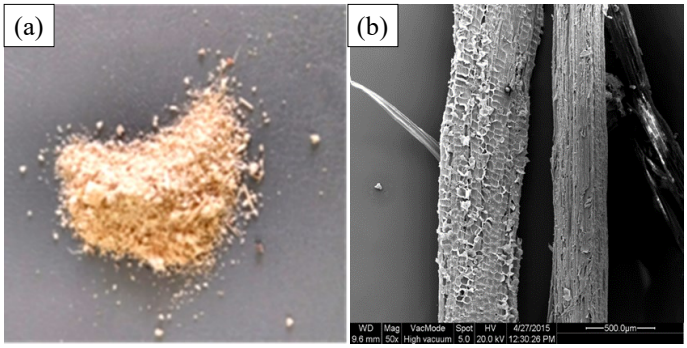

Figure 1. Photograph of (a) dried raw sago pith waste and (b) FESEM micrograph of longitudinal section of sago pith waste.

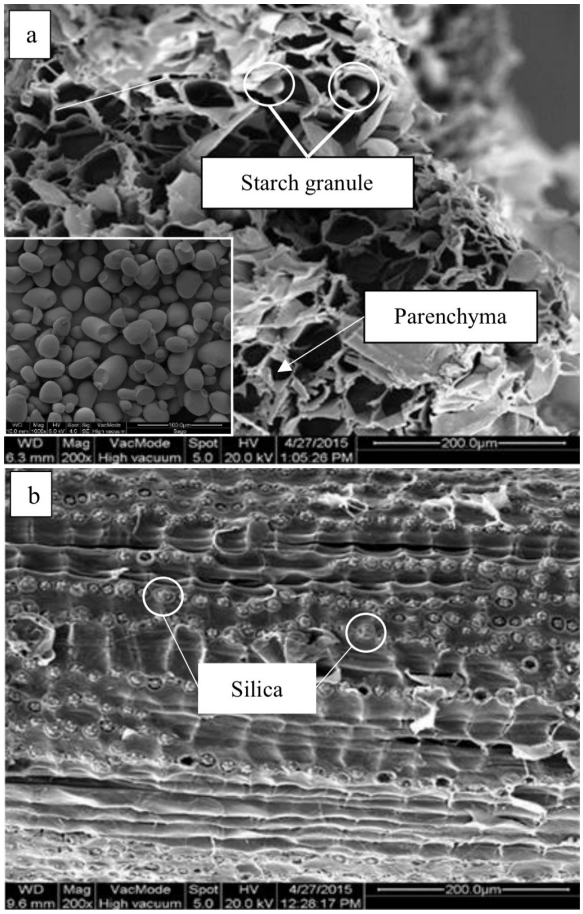

Figure 2. SEM micrograph (a) cross section and (b) longitudinal section of sago pith waste surface at 200× magnification. The embedded micrograph shows the SEM micrograph of sago starch granules at a magnification of 1000×.

The FESEM micrograph of the sago pith waste surface is shown in Figure 2(b). The surface of the sago pith waste appears non-smooth and has an evenly corrugated coating. Sago pith waste showed a bump structure on the surface similar to the findings of the study conducted by Park *et al.* (2003) who used untreated fibers of rice husk ash. According to him, the lump structure found on the surface of rice husk ash fibers is silica and this is equivalent to the lump structure shown by sago pith waste. The presence of silica on the surface of sago pith waste was supported by elemental analysis through EDX spectroscopic analysis as shown in Figure 3. Generally, the existence of silica was detected in plants grown in soils of high mineral content.

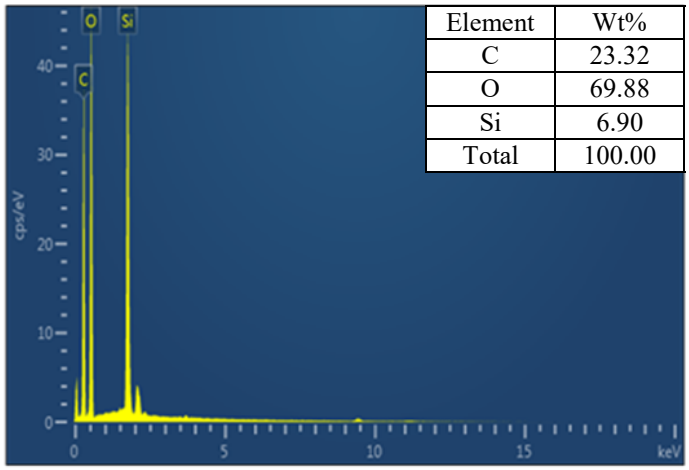

Element	Wt%
C	23.32
O	69.88
Si	6.90
Total	100.00

Figure 3. The EDX spectrum for sago pith waste.

3.3 Fourier Transform Infrared Spectroscopy

Figure 4 displays FTIR spectra for sago pith waste. The broad and intense peak at 3311 cm^{-1} was assigned to the vibration of free O-H groups present in the cellulose I. This peak also corresponded to the intra-and intermolecular hydrogen bonds (Sheltami *et al.* 2012). The band at 2900 cm^{-1} was associated with C-H stretching present in cellulose and hemicellulose. The prominent peak at 1711 cm^{-1} was attributed to the C = O

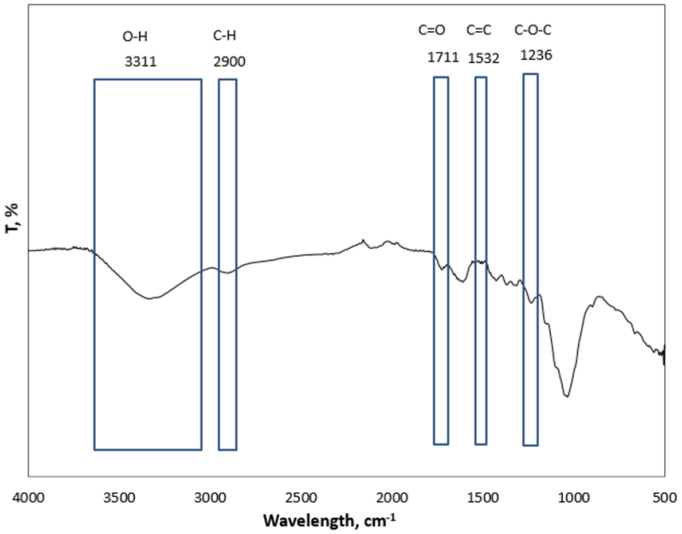

Figure 4. FTIR spectra of sago pith waste

https://doi.org/10.26656/fr.2017.7(S2).13

stretch of the acetyl group and the ester group on hemicellulose and the carboxylic group network on ferulic and *p*-comeric acids in lignin. In the same spectra, the peak at 1532 cm^{-1} represented the C-C aromatic vibration of aromatic rings of lignin. The band at 1236 cm^{-1} corresponds to the C-O-C asymmetric vibration of ether groups. The band at 900 cm^{-1} can be ascribed to the ß-glicosidic bonds between glucose units of amorphous cellulose.

3.4 Thermal properties of sago pith waste

The TGA and DTG thermograms for sago pith waste are shown in Figure 5. The thermogram shows an initial mass decrease in the temperature range of 25°C to 100° C. This was due to the vaporization of absorbed water, the release of moisture and low molecular mass compounds such as extractives (Karimi *et al.* 2014). The second stage of the decomposition process takes place around a temperature of 200 - 300°C. There is a shoulder at around 230°C as shown in DTG thermogram (Figure 5b). The third stage, occurred in the range of 250°C and 375°C, with a maximum degradation temperature of 310°C. According to Coelho de Carvalho *et al.* (2017) this is due to the loss of weight promoted by cellulose decomposition. Thermal decomposition of lignin, hemicellulose and cellulose occurs in the temperature range around 160–900°C, 220–315°C and 315–400°C as described by Yang *et al*. (2007). Each component of lignocellulose, namely cellulose, hemicellulose and lignin have a different chemical structure (Sonia and Dasan, 2013). Thus, the decomposition temperature also varies. Hemicellulose decomposes faster because hemicellulose contains branched chains that are easier to decompose at low temperatures. Cellulose has long polymer chains as well as crystal phases that contain strong inter and intra bonds of hydrogen molecules. Due to this, cellulose is more thermally stable and requires higher energy to decompose than hemicellulose. Whereas the chemical structure of lignin is more complex and has an aromatic ring as well as a larger molecular weight. Therefore, the temperature range of lignin decomposition is higher. The large decomposition temperature range of sago pith waste is due to the overlap of the decomposition peaks of cellulose, hemicellulose and lignin as studied by Chirayil *et al.* (2014).

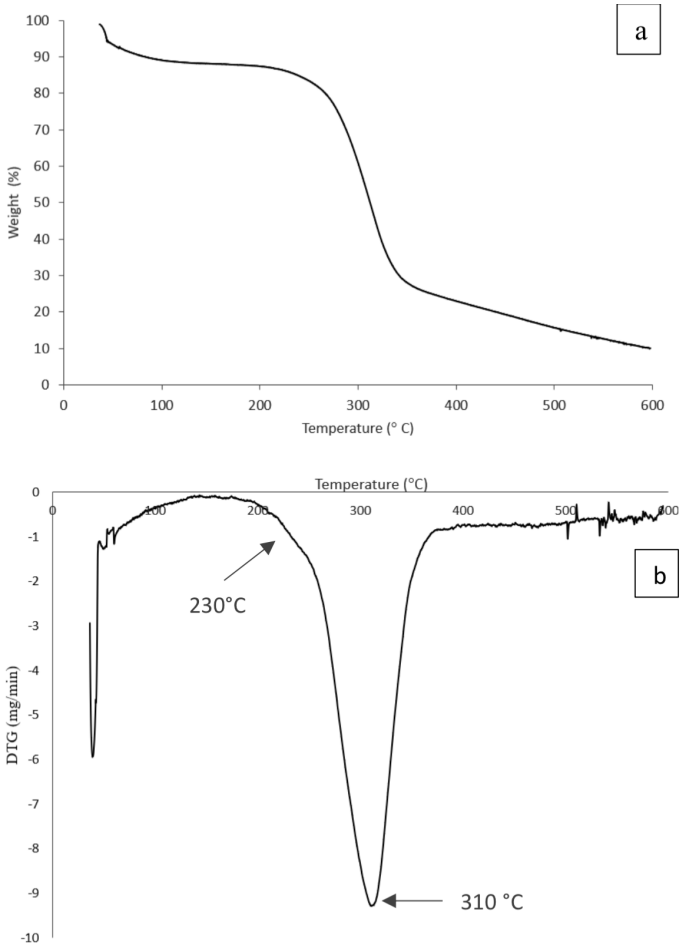

Figure 5. Thermogram of TGA and DTG for sago pith waste.

4. Conclusion

The results of chemical composition showed the highest content of sago pith waste was starch followed by cellulose, hemicellulose and lignin. The fiber morphology observation displayed the average size of sago pith waste was around 300-600 µm. The non-smooth surface indicates the presence of silica. Due to the presence of lignocellulosic fibrous as described in this study, it is expected that sago pith waste can be used for bioethanol production, extraction of cellulose as well as nanocellulose for biocomposite and many more.

Conflicts of interest

The authors declare no conflict of interest.

Acknowledgements

The authors would like to thank the Malaysia Ministry of Higher Education for the financial support on the analysis of data using grant allocation from ERGS/1/2013/STG01/UKM/02/2 and Center for Collaborative Innovation, Universiti Kebangsaan Malaysia through its Dana Inovasi INOVASI-2017-001. Special thanks to the Radiation Processing Technology Division and Industrial Technology Division, Malaysian Nuclear Agency for technical support and equipment facilities.

References

Bujang, K.B. and Ahmad, F.B. (1999). Production and utilization of sago starch in Malaysia. Proceedings of the International Sago Seminar 1999. Sarawak, Malaysia.

Chirayil, C.J., Joy, J., Mathew, L., Mozetic, M., Koetz, J.

https://doi.org/10.26656/fr.2017.7(S2).13

and Thomas, S. (2014). Isolation and characterization of cellulose nanofibrils from *Helicteres isora* plant. *Industrial Crops and Products,* 59, 27–34. https://doi.org/10.1016/j.indcrop.2014.04.020

Coelho de Carvalho Benini, K.C., Voorwald, H.J.C., Cioffi, M.O.H., Milanese, A.C. and Ornaghi Jr., H.L. (2017). Characterization of a new lignocellulosic fiber from Brazil: *Imperata brasiliensis* (*Brazilian Satintail*) as an alternative source for nanocellulose extraction. *Journal of Natural Fibers*, 14(1), 112-125. https://doi.org/10.1080/15440478.2016.1167647

Kamal, M.M., Baini, R., Mohamaddan, S., Ragai, A.H., Fong, L.S., Rahman, N.A., Mili, N., Taib, S.N.L., Othman, A.K. and Abdullah, M.O. (2017). Comparisons of the physicochemical and functional properties of commercially and traditionally processed sago starch. *MATEC Web of Conferences,* 87, 03007. https://doi.org/10.1051/matecconf/20178703007

Karimi, S., Tahir. P.M., Karimi A., Dufresne, A. and Abdulkhani. A. (2014). Kenaf bast cellulosic fibers hierarchy: A comprehensive approach from micro to nano. *Carbohydrate Polymers,* 101, 878–885. https://doi.org/10.1016/j.carbpol.2013.09.106

Lai, J.C., Aizan, W., Abdul, W. and Toh, W.Y. (2014). Mechanical, thermal and water absorption properties of plasticised sago pith waste. *Fibers and Polymers,* 15(5), 971–978. https://doi.org/10.1007/s12221-014-0971-8

Nitta, Y., Nakayama, T. and Matsuda, T. (2006). Structure and function of intercellular spaces in the stem of sago palm: Electron microscopic study. Retrieved from website: https://www.jstage.jst.go.jp/article/jcsproc/223/0/223_0_358/_pdf

Park, B.D., Wi, S.G., Lee, K.H., Singh A.P., Yoon, T.H. and Kim, Y.S. (2003). Characterization of anatomical features and silica distribution in rice husk using microscopic and micro-analytical techniques. *Biomass Bioenergy,* 25(3), 19–327. https://doi.org/10.1016/S0961-9534(03)00014-X

Sheltami, R.M., Abdullah, I., Ahmad, I., Dufrene, A. and Kargarzadeh, H. (2012). Extraction of cellulose nanocrystals from mengkuang leaves (*Pandanus tectorius*). *Carbohydrate Polymers,* 88(2), 772-779. https://doi.org/10.1016/j.carbpol.2012.01.062

Singhal, R.S., Kennedy, J.F., Gopalakrishnan, S.M., Kaczmarek, A., Knill, C.J. and Akmar, P.F. (2008). Industrial production, processing and utilization of sago palm-derived products. *Carbohydrate Polymers,* 72(1), 1-20. https://doi.org/10.1016/j.carbpol.2007.07.043

Sonia, A. and Dasan, K.P. (2013). Chemical, morphology and thermal evaluation of cellulose microfibers obtained from *Hibiscus sabdariffa*. *Carbohydrate Polymers*, 92(1), 668–674. https://doi.org/10.1016/j.carbpol.2012.09.015

Wise, L.E., Murphy, M. and D'Addieco, A.A. (1946). Chlorite, holocellulose, its fractionation and bearing on summative wood analysis and on studies on the hemicellulose. *Paper Trade Journal*, 122(2), 35–43.

Yang, H., Yan, R., Chen, H., Lee, D.H. and Chuguang, Z. (2007). Characteristics of hemicellulose, cellulose and lignin pyrolysis. *Fuel*, 86(12-13), 1781–1788. https://doi.org/10.1016/j.fuel.2006.12.013

https://doi.org/10.26656/fr.2017.7(S2).13